COMPUTATIONAL MODEL OF THE CONTRACTION CAUSED BY THE POLYMERIZATION OF BULK FILL DENTAL RESIN AND EXPERIMENTAL VALIDATION

Claudio A. Junior

Emílio G. F. Mercuri

cantunes.j@gmail.com

emilio@ufpr.br

Universidade Federal do Paraná

Rua Evaristo F. F. da Costa nº 418, 80050-540, Paraná, Curitiba, Brazil

Ana Paula G. O. Franco

anapaula.gebert@gmail.com

Universidade Tecnológica Federal do Paraná

Avenida Sete de Setembro nº 3165, 80230-901, Paraná, Curitiba, Brazil

Leandro Z. Karam

leandro.karam@pucpr.br

Pontifícia Universidade Católica do Paraná

Rua Imaculada Conceição nº 1155, 80215-901, Paraná, Curitiba, Brazil

Manoella Costa

costa.manoella@hotmail.com

Universidade Estadual de Ponta Grossa

Rua Coronel Bittencourt nº 689, 84010-290, Paraná, Ponta Grossa, Brazil

Abstract. *The objective of this work is to propose a computational study of the polymerization strains in dental resins which can cause several problems in orthodontic treatments. This is done by the development of a finite element analysis and the comparison with a laboratorial experiment of the contraction caused by the polymerization of bulk fill dental resins. Once the numerical model is validated, it can be used to vary the resin apposition and light exposition* *patterns in different scenarios at low cost, quick response and without harm to people under treatment. High contraction stresses on light-activated composites, can cause adhesive interface failure. This undesirable defect may lead to micro-infiltration, and, consequently, the development of marginal caries, postoperative sensitivity and pulp damage. The laboratory experiment was performed in third human molars, in which was installed an optical fiber recorded with two fiber Bragg grating that function as two sensors with different wavelengths that measure temperature and strain. For the computational experiment, a three-dimensional geometrical model of a first human molar obtained via CT Scan was created to mimic the experiment. The mesh convergence study and simulation were performed in Ansys software using a thermo-elastic constitutive model. The temperature measured in the laboratory was used as an input data representing a thermal load in the numerical model of the resin. The results are promising, considering that the computational model is at initial stage, the resin strains in the gingival-occlusal direction versus time curve of the model has the same shape as the experiment, but the magnitude is quite different. Further improvement will be done such as a more realistic geometrical model and the use of a viscoelastic theory for the mechanical response of the resin.*

Keywords: *Dental composite resins, FEM, Polymerization, Thermo-elastic model, Contraction.*

1 INTRODUCTION

The high contraction of the composite resins caused by the polymerization can cause failures at the resin-dentin interface. This undesirable defect may lead to micro-infiltration, and, consequently, the development of marginal caries, postoperative sensitivity and pulp damage. Even the displacement of the applied material can occur (Lutz et al., 1991).

These problems generate economic impacts due to the necessity of investments that are required to restore the damaged tooth, both for the patient as well as for the dental plans due to the repetition that may be required to perform the dental treatment.

The objective of this work is to propose a computational study of the polymerization strains in dental resins which can cause several problems in orthodontic treatments. The authors develop a computational experiment to compare it with a laboratorial experiment that measures the contraction of the dental resin during its polymerization.

Once the numerical model is calibrated and validated, it can be used to study the variation the resin apposition and light exposition patterns, some critical procedures during the restoration process. These different scenarios at an *in silico* model represent benefits such as low cost, quick response and no harm to people being under treatment.

2 LITERATURE REVIEW

Some studies are based on the finite element analysis along with the digital-image-correlation technique, with that combination were found some important data for the area of dentistry, more specific the area of restoration.

Chuang (2011), using both techniques, found that the cavity with 2 mm (width) x 4 mm (diameter) had the maximum von Mises and principal stresses located at the cavity floor, indicating a high risk of adhesive failure on the cavity floor, caused by the formation of contraction stress. Using the same methodology Chuang (2016) stated that the problems that may occur at the restoration local are influenced by the direction and intensity of the light used to cure the resin. Chen (2014) declared that the light energy density when in high concentration was the one responsible to inflect the stress, with that the curing by steps would decrease the stress.

A model that can be applied to the finite element method, was formulated by Petrovic (2007) the model is that the shrinkage strain can be represented by a diffusion type equation. With the use of linear viscoelasticity, they were able to determine that the stresses in the polymer caused by the shrinkage, and that the maximum stresses are in the beginning of the polymerization, when the temperature is higher.

2.1 Thermo-elastic model

The model that was used in this work is based on the Hooke 3D's law plus the isotropic thermo-elastic effects. The variation of temperature ΔT has a volumetric influence in the stress level. Eq. 1 shows the relation between strain and stress.

$$\sigma_{ij} = C_{ijkl}(\varepsilon_{kl}^{e} - \varepsilon_{kl}^{T}) = C_{ijkl}(\varepsilon_{kl}^{e} - \alpha\Delta T\delta_{kl}) \quad (1)$$

Proceedings of the XXXVIII Iberian Latin-American Congress on Computational Methods in Engineering
P.O. Faria, R.H. Lopez, L.F.F. Miguel, W.J.S. Gomes, M. Noronha (Editores), ABMEC, Florianópolis, SC, Brazil, November 5-8, 2017.

In the previous equation C_{ijkl} is the fourth-order stiffness tensor, α is the isotropic coefficient of thermal expansion, both based on materials properties. The symbols ε_{kl}^{e} and ε_{kl}^{T} are the second-order elastic strain and thermal strain tensors, σ_{ij} is the second-order stress tensor and δ_{kl} is de Kronecker delta tensor (Radovitzky et al., 2013).

3 MATERIALS AND METHODS

The laboratory experiment was performed at the thermography laboratory of the Federal Technological University of Paraná (UTFPR), which has a controlled temperature of 21 ºC. For the experiment were used 15 samples of third human molars without the presence of caries, in which a 4x4x4 mm cavity was created and two through holes perpendicular to each other at 2 mm and 3 mm from the bottom of the cavity. In these holes was inserted an optical fiber recorded with two fiber Bragg grating that function as two sensors with different wavelengths that measure temperature and strain. The two sensors were installed in directions perpendicular to each other and one of them was inserted in a hypodermic needle to isolate the effect of the strain. After the tooth preparation, the cavity was filled using Filtek Fill Flow resin (3M / ESPE) which was photoactivated for 10 seconds with the LED device (Vallo Cordless/Ultradent). A photograph of the tooth already restored with the optical fibers is illustrated in Fig. 1.

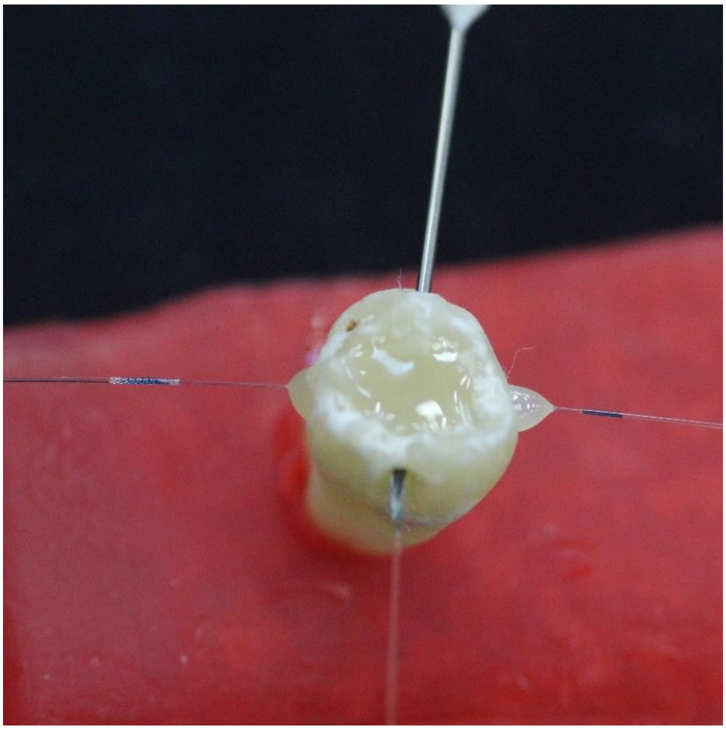

Figure 1. Photograph of the laboratory experiment

The sensor at 2 mm from the bottom of the cavity measured the strain and temperature, while the sensor 3 mm from the bottom of the cavity that was inside the needle measured only the temperature. The data was recorded each 0.5 second for one hour and analyzed statistically and converted to temperature and strain. One of the 15 samples of third human molars from the experiment was chosen for the computational experiment. The authors chose the smoothest curves with the median values compared to the other trials of the laboratory experiment samples. This choice is depicted in Fig. 2 and 3.

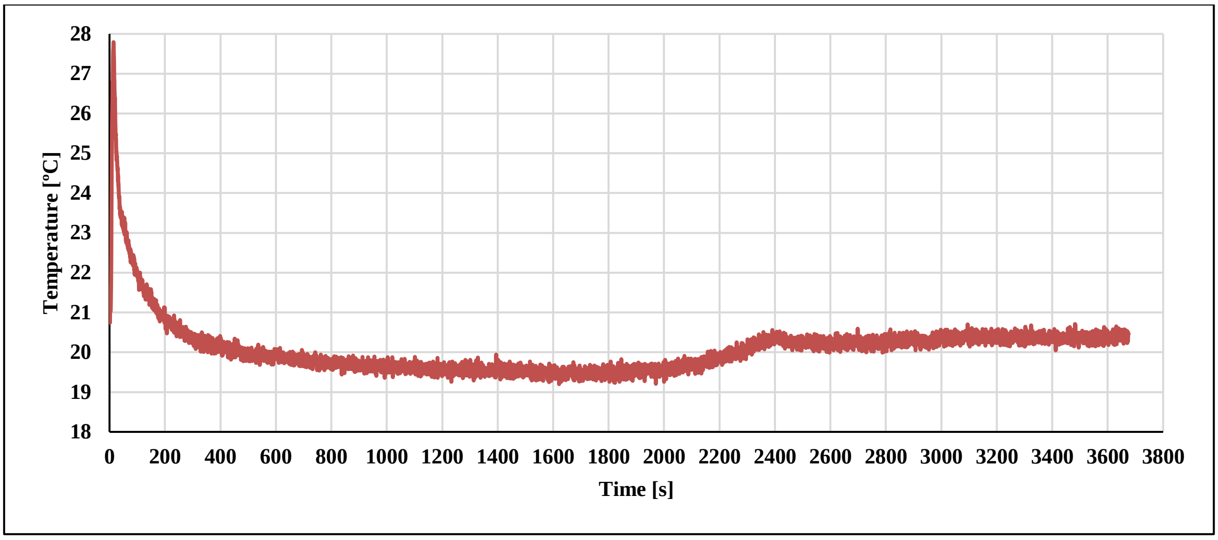

Figure 2. Temperature evolution measured during polymerization

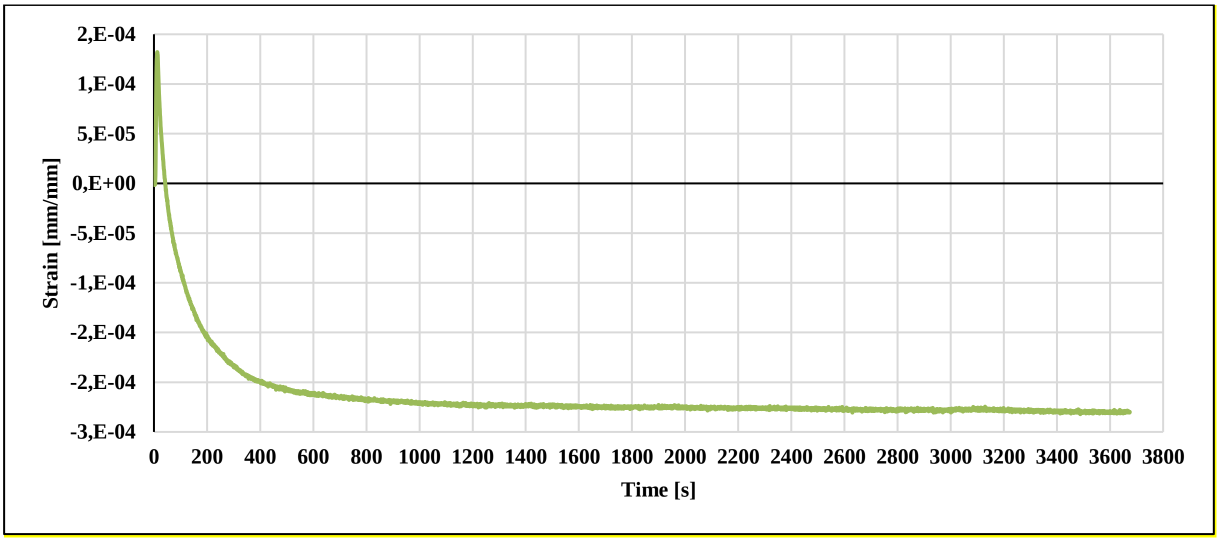

Figure 3. Strain evolution measured during polymerization

A three-dimensional model of a first human molar obtained by a CT scan was used. By the tools of FreeCad software, a 4x4x4 mm cavity was created with the initial point at the middle point of the top surface of the tooth. After this, the cavity was filled with the model of the dental resin which has the top surface equal as the one on the full model of the tooth. The model needed a base so it can be fixed, for that a model that simulate the cortical bone was created. The complete model with the three components is showed at Fig. 4. It is important to emphasize that the model described below is in the initial state and is simplified, it will be improved in the future with the addition of a viscoelastic model for the mechanical response of the resin and the

CT scan of the same tooth that were used in the laboratory experiment. The tooth used in the simulation is a generic first human molar obtained from CT scan.

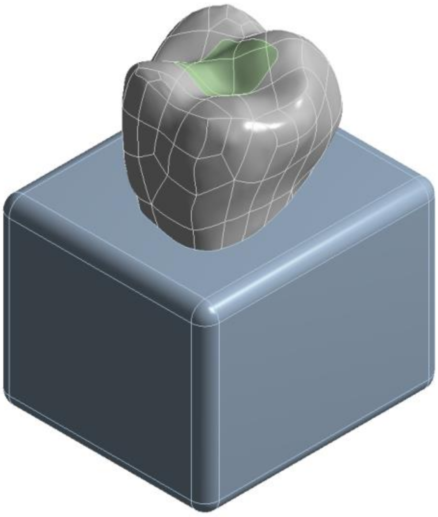

Figure 4. Complete model (first molar + dental resin + cortical bone)

Using the complete model, a static structure analysis using the finite element method was performed with the software Ansys. To begin the analysis, the properties of the components have been defined as shown in Table 1. These were considered as isotropic elastic materials. The coefficients of thermal expansion that were used are mean values, because the used model of the tooth is only one material, it is not being considered the enamel, pulp, cement and ligaments. As well as the base for the tooth that is only the cortical bone without the consideration of the trabecular bone.

Table 1. Properties of the components materials

Material	Young Modulus E [MPa]	Poisson Coefficient ν	Coefficient of Thermal Expansion [°C^{-1}]
Dentin	18600[a]	0,31[a]	20E-5[c]
Cortical Bone	13700 [a]	0,30[a]	10E-5[d]
Dental Resin	3000[b]	0,25[b]	5E-5[c]

[a] Boccacio, et al., 2006. [b] Xu, et al., 1999. [c] Alnazzawi, et al., 2012. [d] Ranu, 1987.

Then the contact regions of the components were delimited, which are between the tooth roots and the cortical bone and between the tooth cavity and the dental resin. These regions are shown in Fig. 5.

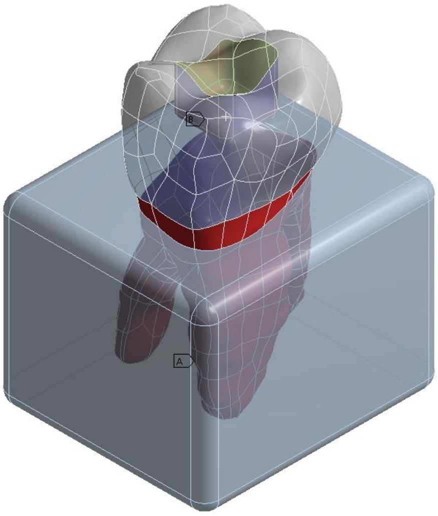

Figure 5. Contact regions

The thermal load applied only to the resin model was based on the evolution of the temperature that was measured by one of the sensors on the laboratory experiment shown in Fig. 2. However as in the experiment the temperature was measured every half a second for one hour, that is, more than 7000 measurements were made. Due to this it was decided to use the temperature data every two seconds.

The model that represents the cortical bone had its inferior face fixed according to the Fig. 6.

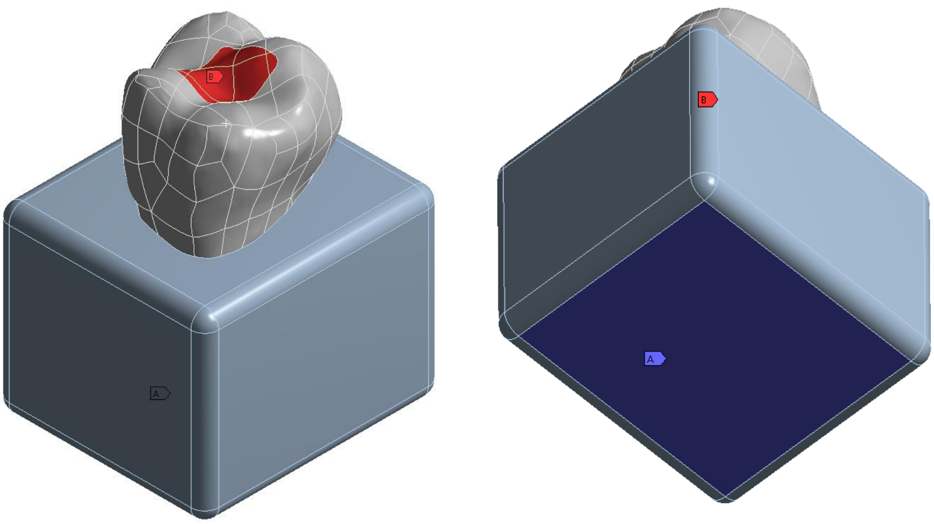

Figure 6. Area of the thermal load application and the fixation of the cortical bone

For the mesh, it was used the Tetrahedrons method with the element size of 1 mm and the element order as quadratic. The mesh parameters were based on the work done recently (Antunes Junior, 2017) with the same model, but for the chewing force. The mesh can be seen in the Fig. 7.

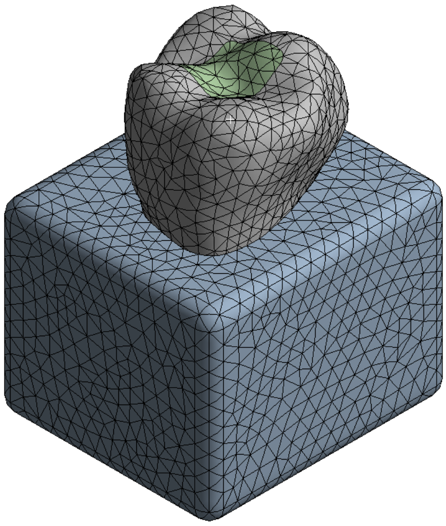

Figure 7. Mesh model

For the analysis to be similar to the laboratory experiment a probe was created at 2 mm from the bottom of the resin model, to simulate the optical fiber with the Bragg net. The probe was created so that the results of the strain of the computational analysis can be compared with the laboratory experiment. In Fig. 8 the axes represent the position of the probe.

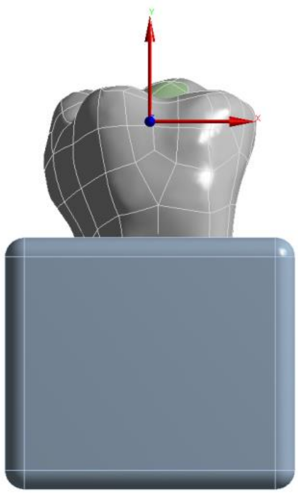

Figure 8. Probe representation

After all this preparation, the system equations of the thermo-elastic model is solved, obtaining the strain suffered by the probe.

In addition to the strain analysis in the probe, the maximum and the minimum principal stresses were checked at each of the interfaces between the tooth and the resin. The red line shown in Fig. 9 represents three of the five faces that were used.

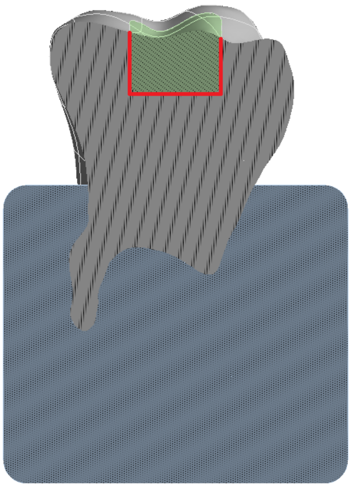

Figure 9. Interfaces between the tooth and the resin

The computer used to solve the model has the following configuration: i3-4160 @ 3.6 GHz; 8gb of ram; AMD 7850 2GB. The execution time of each analysis was on average of 4 hours and 40 minutes.

4 RESULTS

Before determining the properties of the materials and the boundary condition that would be used in the model, tests were performed in the first 200 seconds of the application of the thermal force. In each test, there was one change at a time, being maintained for the following tests. As can be seen in Fig. 10, the change in the coefficient of thermal expansion of the resin generated the greatest impact on the result.

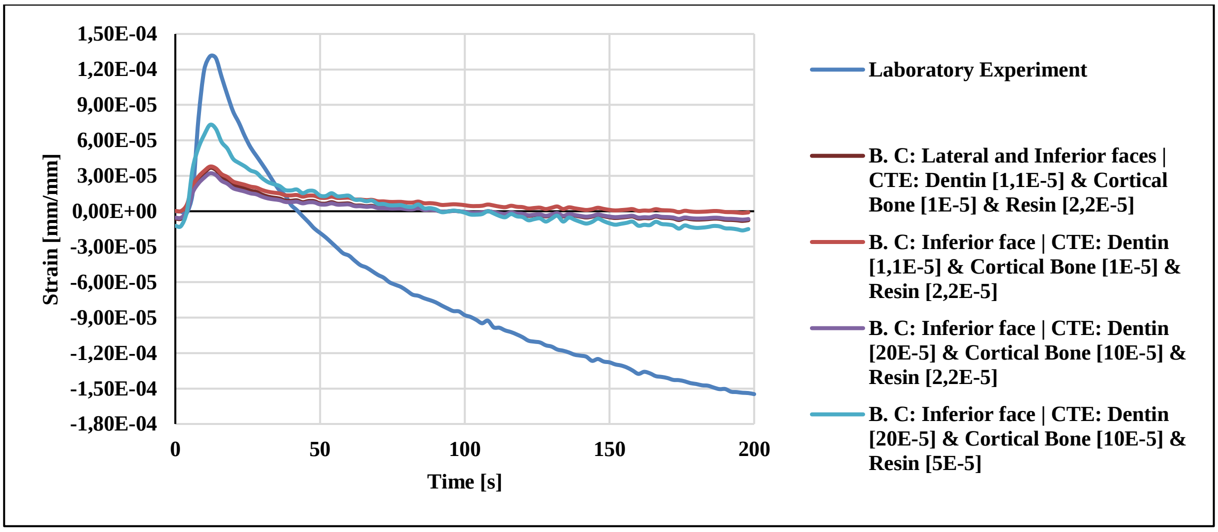

Figure 10. Results of the tests changing the properties values

Based on the computational model described previously, the result found for the strain on the probe and the strain data from the laboratory experiment were set out in the Fig. 11.

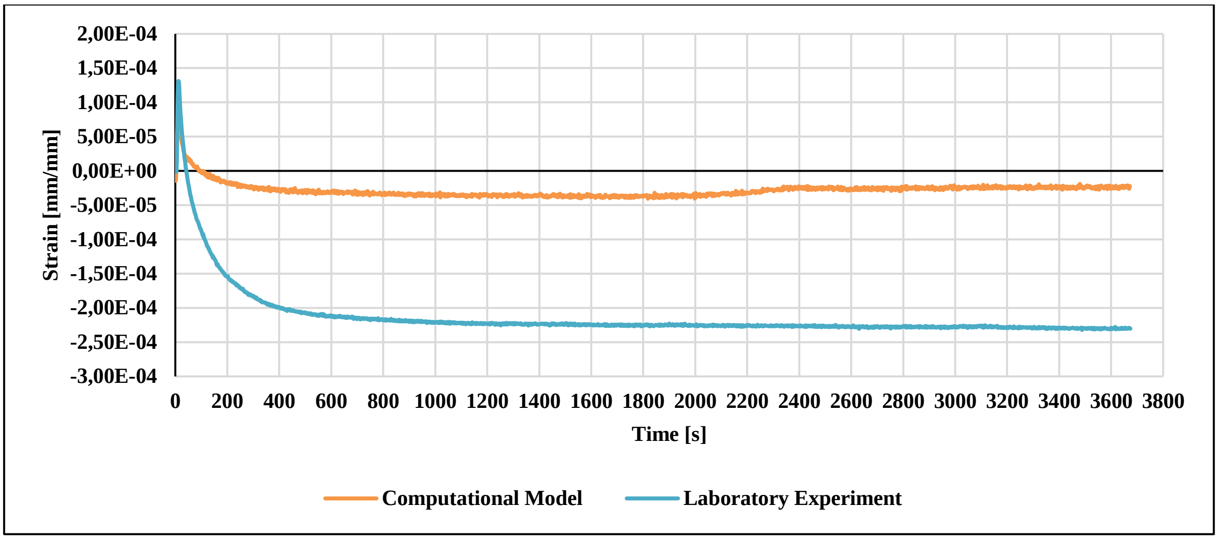

Figure 11. Comparison of the strain evolution

As can be seen the strain achieved by the computational model for the analyzed time space presents the same curve shape of the strain found at the laboratory experiment. The curve shows a decrease in the strain from the 2000 seconds mark till the end of the measurement. After 2000 seconds the strains tend to return to zero because the resin temperature is returning to the ambient temperature, which is 21 ºC, and the material model used is simply elastic. In the experiment, the temperature falls below 21 ºC because of the entropy changes that occur in the thermal degradation of polymers.

Table 2. Maximum and minimum principal stresses on the resin faces

Face	Compression [MPa]	Traction [MPa]
1	- 2,2821 [a]	1,1108 [b]
2	- 2,3768 [a]	1,1569 [b]
3	- 2,7545 [a]	1,3408 [b]
4	- 2,2499 [a]	1,0951 [b]
5	- 1,3808 [a]	0,6721 [b]

[a] Time of 12 seconds. [b] Time of 1818 seconds.

Table 2 show the maximum values for the compression and traction stresses during the thermal load, respectively, on the faces of the resin. In the time of 12 seconds, the maximum compression occurs, given the fact that the resin is in a state of expansion due to the increase in temperature, the faces are being compressed relative to the faces of the tooth cavity. In the same way, as in 1818 seconds the temperature is in a state of stability, so the resin is returning to its original form, so a traction is happening in the faces of the resin.

It is possible to verify the stress distribution after the end of the application of the thermal load on the five faces of the resin with the Fig. 12 to 21. The distribution can aid in determining where the material rupture can occur.

The four lateral faces showed little variation of maximum and minimum stress between them and the distributions were similar in the faces. In the maximum principal stress analysis, the highest stress was presented near the upper corners and the lowest stress in a lower range close to the bottom. And for the minimum principal stress analysis the distribution of the stresses is that the highest stress has a band near the bottom and the lowest stress a band in the upper part of the resin face.

The bottom face of the resin showed a similar distribution between the maximum and minimum principal analysis, being that the maximum stress is on the corners and the minimum stress is on the center.

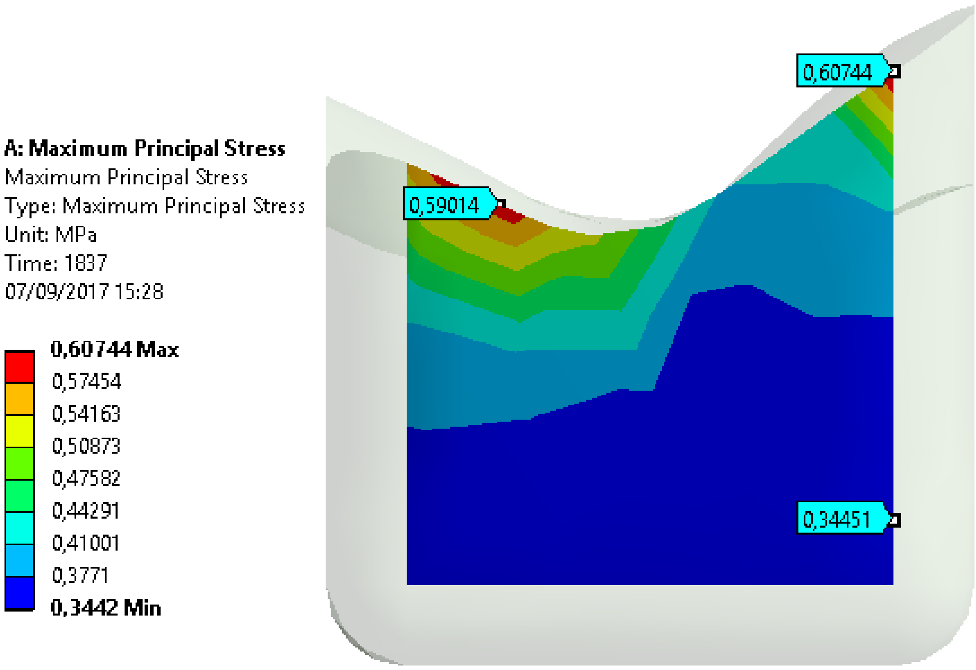

Figure 12. Maximum principal stress – face 01

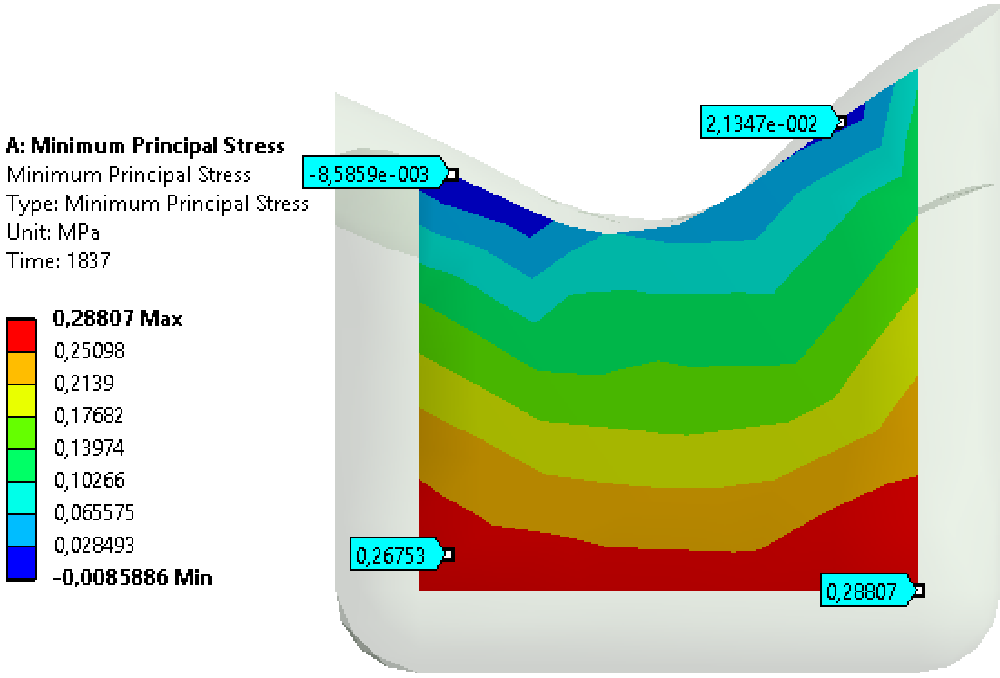

Figure 13. Minimum principal stress – face 01

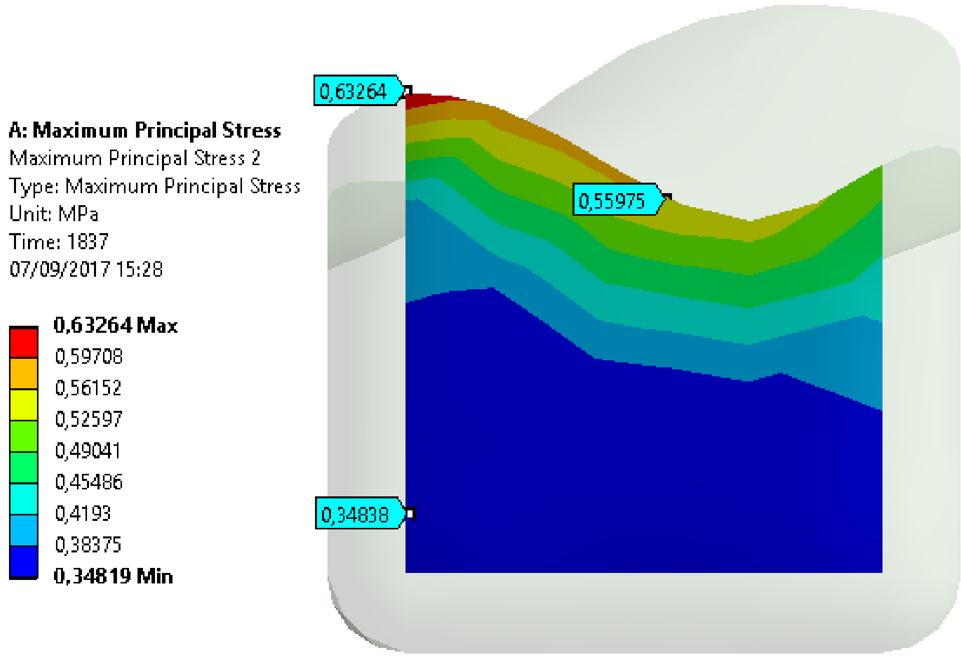

Figure 14. Maximum principal stress – face 02

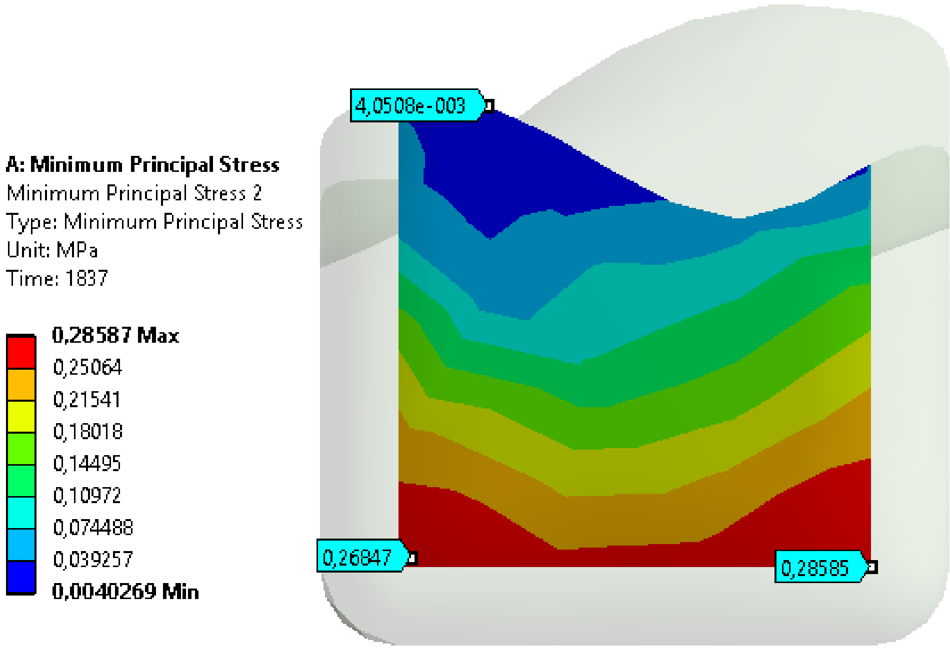

Figure 15. Minimum principal stress – face 02

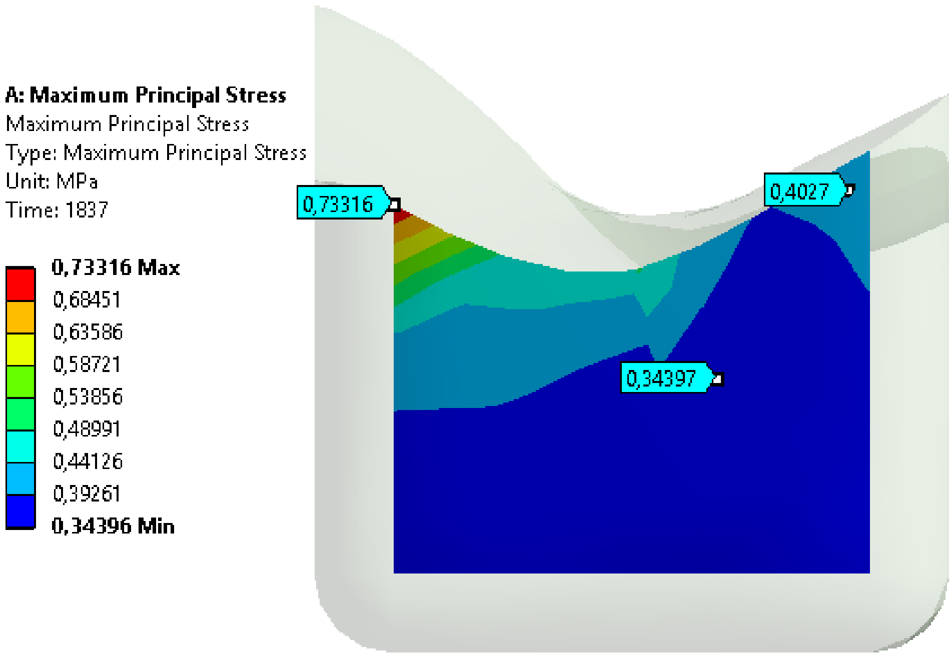

Figure 16. Maximum principal stress – face 03

Proceedings of the XXXVIII Iberian Latin-American Congress on Computational Methods in Engineering
P.O. Faria, R.H. Lopez, L.F.F. Miguel, W.J.S. Gomes, M. Noronha (Editores), ABMEC, Florianópolis, SC, Brazil, November 5-8, 2017.

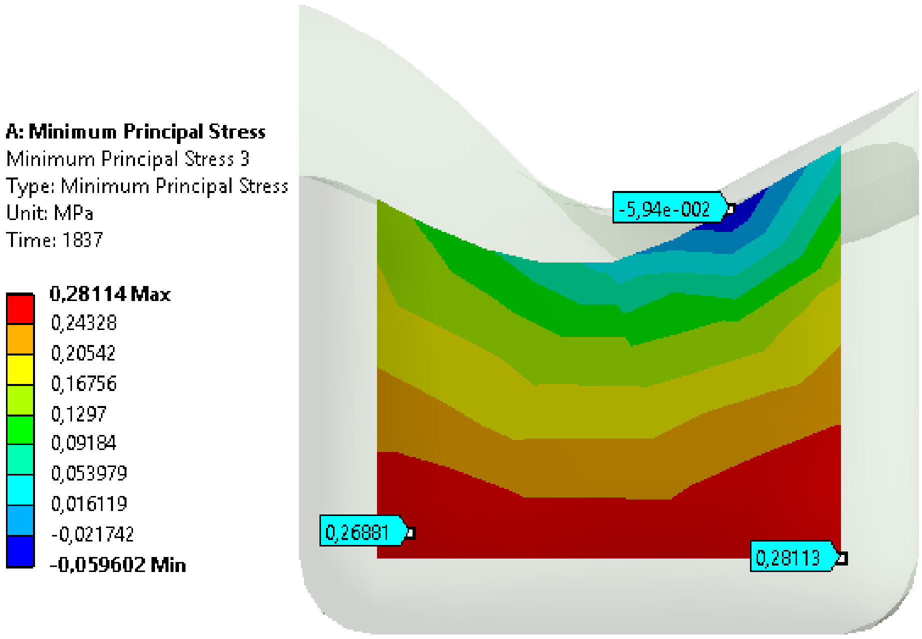

Figure 17. Minimum principal stress – face 03

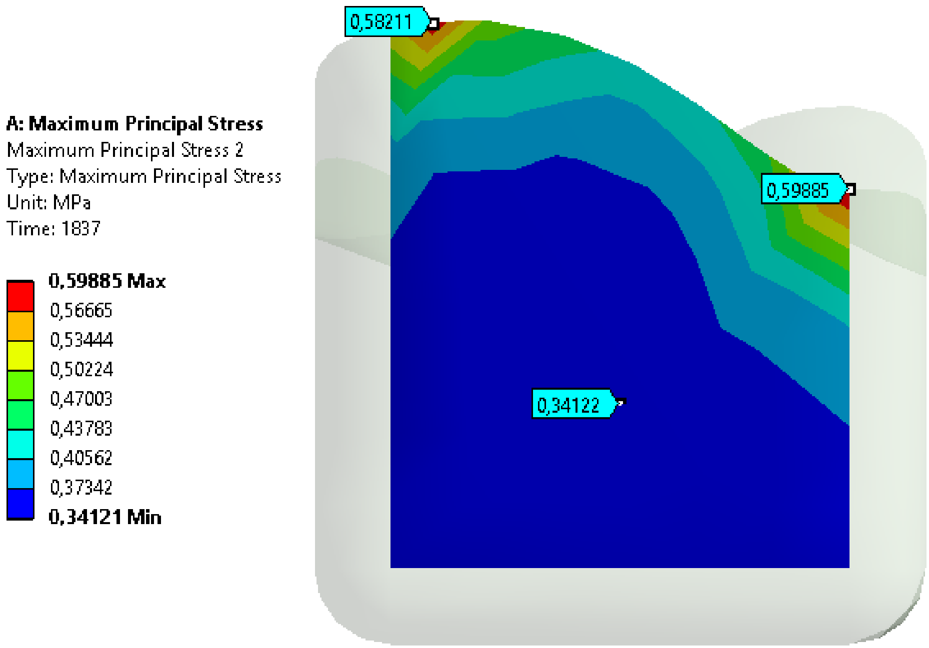

Figure 18. Maximum principal stress – face 04

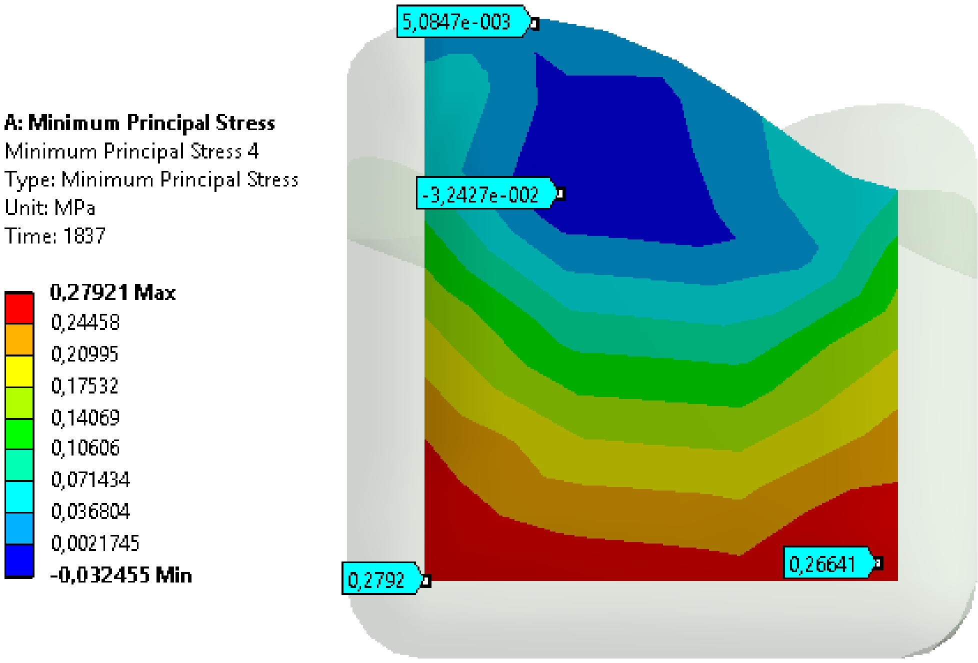

Figure 19. Minimum principal stress – face 04

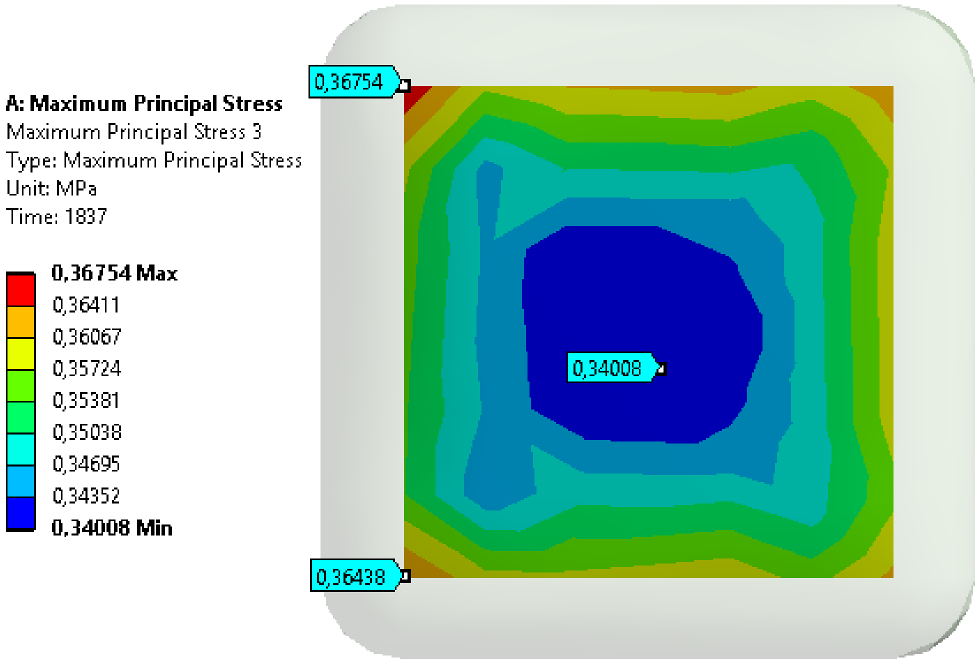

Figure 20. Maximum principal stress – face 05

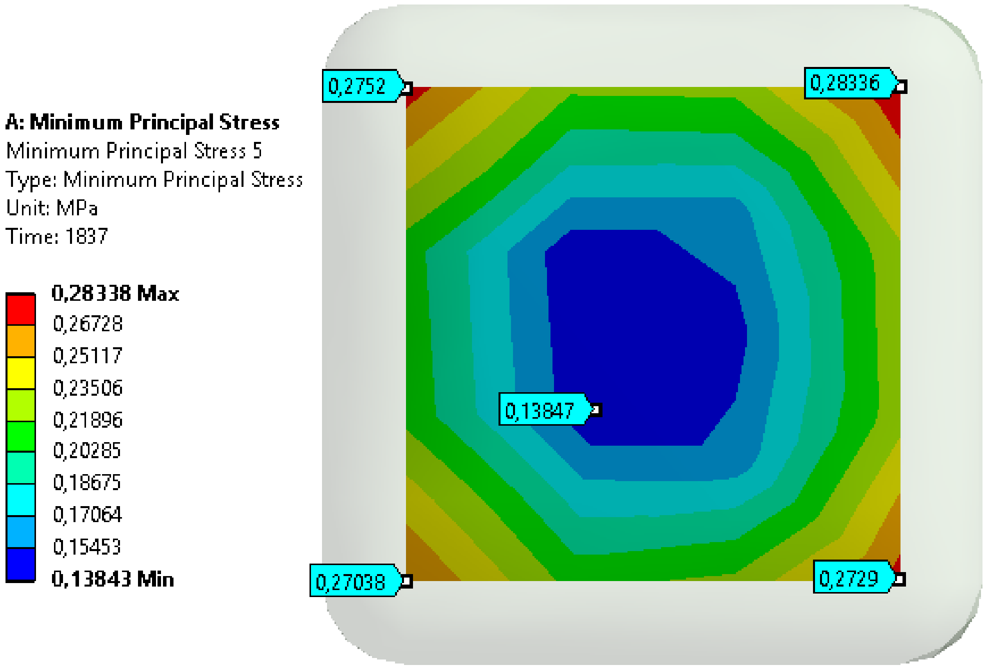

Figure 21. Minimum principal stress – face 05

5 CONCLUSION

Although the objective of simulating the laboratory experiment was not fully achieved, the presented results represented the influence of a temperature variation in the resin. One of the reasons why the numerical results did not reach the experiment is that the thermal load is based on the temperature values that were measured by the sensor in the center of the resin and does not represent the wave front process of the polymerization triggered by the LED Device. The model revealed the rapid expansion and after it a contraction behavior that is expected for a thermo-elastic model. For future improvements, it will be applied the viscoelastic model for resin constitutive response. Furthermore, the authors have the intention to apply the model for other dental resins and other resin application procedures, with the objective of improving the orthodontic practice of use of resins in restorative processes. In general, this work contributes to study how the failure in the adhesive interface between the tooth and the resin happen, an effort made to avoid such a phenomenon and to prevent unnecessary expenses.

ACKNOWLEDGEMENTS

The authors would like to acknowledge the financial support from the Coordination for the Improvement of Higher Education Personnel (CAPES), the Post-Graduate Program in Numerical Methods in Engineering (PPGMNE/UFPR) and the Laboratory of Thermography of UTFPR.

REFERENCES

Alnazzawi, A., & Watts, D. C., 2012. Simultaneous determination of polymerization shrinkage, exotherm and thermal expansion coefficient for dental resin-composites. *Dental Materials*, vol. 28, n. 12, pp. 1240-1249.

Antunes Junior, C., & Mercuri, E. G. F., 2017. Estudo de convergência de malha para modelo representative de molar submetido a cargas de mastigação. *Simpósio de Métodos Numéricos em Engenharia, Curitiba. Universidade Federal do Paraná (article submitted to the congress in 18/08/2017).*

Boccacio, A., Lamberti, L., Pappalettere C., Carano, A., & Cozzani, M., 2006. Mechanical behavior of an osteotomized mandible with distraction orthodontic devices. *Journal of Biomechanics*, vol. 39, n. 15, pp. 2907-2918.

Chen, T. Y. F., Huang, P. S., & Chuang, S. F., 2014. Modeling dental composite shrinkage by digital image correlation and finite element methods. *Optics and Lasers in Engineering*, vol. 61, pp. 23-30.

Chuang, S. F., Chang C. H., & Chen T. Y. F., 2011. Contraction behaviors of dental composite restorations – finite element investigation with DIC validation. *Journal of the Mechanical Behavior of Biomedical Materials*, vol. 4, n. 8, pp. 2138-2149.

Chuang, S. F., Huang, P. S., Chen, T. Y. F., Huang, L. H., Su, K. C., & Chang, C. H., 2016. Shrinkage behaviors of dental composite restoration – the experimental-numerical hybrid analysis. *Dental Materials*, vol. 32, n. 12, pp. 362-373.

Lutz, F., Krejci, I., & Barbakow, F, 1991. Quality and durability of marginal adaptation in bonded composite restorations. *Dental Materials*, vol. 7, n. 2, pp. 107-113.

Petrovic, L. M., & Atanackovic, T. M., 2008. A model for shrinkage strain in photo polymerization of dental composites. *Dental Materials*, vol. 24, n. 4, pp. 556-560.

Radovitzky, R. Hautefeuille, M. Jean, A., Rosolém, A., & Becker, G., 2013. Structural mechanics: module 3. Available at: http://web.mit.edu/16.20/homepage/3_Constitutive/Constitutive_files/module_3_no_solutions.pdf. Accessed 27 Aug. 2017.

Ranu, H. S., 1987. The thermal properties of human cortical bone: an in vitro study. *Journal of Engineering in Medicine*, vol. 16, n. 3, pp. 175-176.

Xu, H. H. K., Martin, T. A., Antonucci, J. M. & Eichmiller, F. C., 1999. Ceramic whisker reinforcement of dental resin composites. *Journal of Dental Research*, vol. 78, n. 2, pp. 706-712.